Modeling and simulation of 5-axis milling processes

E. Budak (2)*, E. Ozturk, L.T. Tunc

Faculty of Engineering and Natural Sciences, Sabanci University, Istanbul, Turkey

ARTICLE INFO

Keywords:
Milling
Force
Stability

ABSTRACT

5-axis milling is widely used in machining of complex surfaces. Part quality and productivity are extremely important due to the high cost of machine tools and parts involved. Process models can be used for the selection of proper process parameters. Although extensive research has been conducted on milling process modeling, very few are on 5-axis milling. This paper presents models for 5-axis milling process geometry, cutting force and stability. The application of the models in selection of important parameters is also demonstrated. A practical method, developed for the extraction of cutting geometry, is used in simulation of a complete 5-axis cycle.

1. Introduction

5-axis milling has become a widely used process due to its ability to machine complex surfaces. In most of these applications high productivity is required due to the cost of machine tools and parts. Productivity and quality in 5-axis milling can be increased using process models. However, unlike other processes, modeling of 5-axis milling has been very limited. The objective of this paper is to demonstrate selection of process parameters in 5-axis milling for increased productivity using process models and simulations.

Altintas and Engin [1] modeled the cutting edge for generalized milling cutters, and used it in cutting force and stability calculations in 3-axis milling which can be extended to 5-axis milling. However, all process models require tool–part engagement boundaries which are more complicated in 5-axis milling due to the additional degrees of freedom. The calculation of engagement limits in 5-axis milling has been mainly done using non-analytical methods. For example, Larue and Altintas [2] used ACIS [3] solid modeling environment to determine the engagement region for force simulations of flank milling. Kim et al. [4] determined the engagement region using Z-mapping. Ozturk and Budak [5], on the other hand, determined the engagement regions analytically, and modeled the cutting forces and tool deflections.

Chatter is one of the main limitations in 5-axis milling. Although chatter stability in milling has been extensively studied analytically [6–8] and by simulations [9], this has been very limited for ball-end milling and 5-axis milling processes. Altintas et al. [10] extended the analytical milling stability model to the ball-end milling whereas Ozturk and Budak [11,12] included the effect of lead and tilt angles using single- and multi-frequency methods.

Force and the stability models can be used both in planning and analysis. In planning phase, better process parameters can be selected through simulations. In 5-axis milling, however, process parameters may continuously vary along the tool path. In this study, these parameters are obtained using a procedure [13] developed for extraction of milling conditions from cutter location (CL) data. As all CAD/CAM software provides CL files, this approach presents a practical method for integration of the models with the CAD/CAM systems.

In the next section, the geometry of 5-axis milling is briefly introduced together with the force model. The application of the model in lead and tilt angle selection is also demonstrated. For chatter stability analysis of 5-axis milling, single- and multi-frequency solutions are summarized, and used for generation of stability diagrams. The last section of the paper presents simulation of 5-axis milling cycles with example cases.

2. Process geometry and force model

Compared with conventional milling operations, 5-axis milling geometry is more complicated due to the additional degrees of freedom. In this section, 5-axis milling geometry is presented briefly. A more detailed analysis can be found in [5]. Three coordinate systems are used in modeling of 5-axis milling processes. MCS is a fixed coordinate system on the machine tool. TCS consists of the tool axis and two perpendicular transversal axes (x) and (y). FCN consists of the feed, F, the surface normal, N and the cross-feed, C, directions (Fig. 1). The lead angle is the rotation of the tool axis about the cross-feed axis, whereas the tilt angle is the rotation about the feed axis with respect to the surface normal. Lead and tilt angles together with ball-end mill geometry, cutting depth and step over determine the engagement region between the cutting tool and workpiece. In Fig. 1, engagement region, variation of start (φ_{st}) and exit angles (φ_{ex}) along the tool axis are demonstrated for a representative case.

The cutting tool is divided into differential cutting elements to determine the varying engagement boundaries (Fig. 1). The engagement model [5] is used to determine the elements that are in cut. Differential cutting forces in radial, tangential and axial directions shown in Fig. 2 are calculated in terms of the local chip thickness and width, and the local cutting force coefficients. Local chip thickness and cutting force coefficients are variable along the cutting flute depending on the immersion angle φ and z coordinate as presented in Fig. 3.

* Corresponding author.

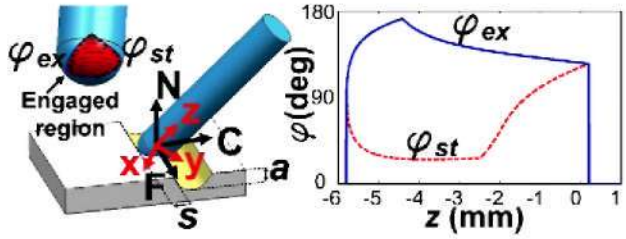

Fig. 1. Engagement region, start and exit angles.

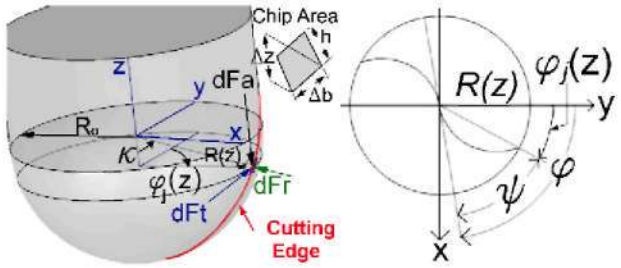

Fig. 2. Tool geometry and differential cutting forces.

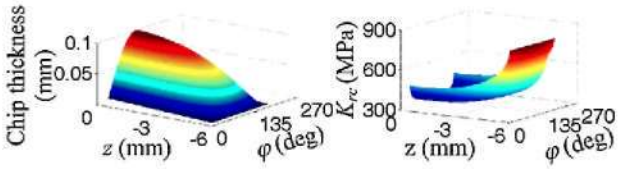

Fig. 3. Chip thickness and force coefficient variation.

Cutting forces, torque and power are calculated by integrating the differential forces within the engagement region. Tool deflections are calculated using the structural properties of the cutting tool and forces at surface generation points [5].

2.1. Force model results

The force model was verified with more than 70 cutting tests [5]. The force model can be used in the selection of lead and tilt angles. The effect of lead and tilt angles on the maximum transversal cutting force, F_{xy}^{max}, is simulated for a representative following-cut case in Fig. 4. The cutting depth and the step over are 5 mm, the feed rate is 0.05 mm/tooth, the spindle speed is 1000 rpm and cross-feed direction [5] is negative. A 12 mm-diameter, two-fluted ball-end mill with 30° helix and 8° rake angle is used. The workpiece material is Ti6Al4V which is commonly used in aerospace industry. Three different lead and tilt combinations are selected in Fig. 4, and the simulations are verified by cutting tests. Comparison of measured and simulated F_{xy}^{max} is given in Fig. 4. The variation of measured and simulated cutting forces in x, y and z directions for one revolution of

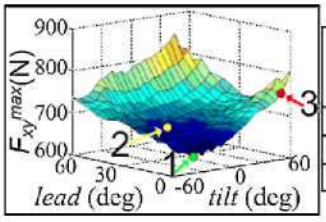

Point	Lead,tilt (deg)	Sim. F_{xy}^{max} (N)	Meas. F_{xy}^{max} (N)
1	0, -40	637	600
2	30, -15	672	652
3	0, 50	752	712

Fig. 4. Simulated and measured cutting forces.

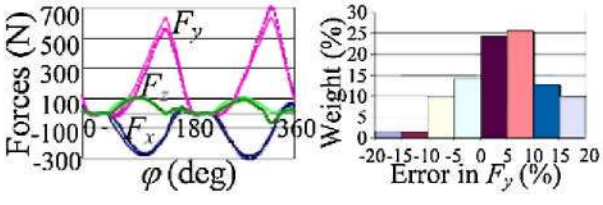

Fig. 5. Predicted forces and error distribution.

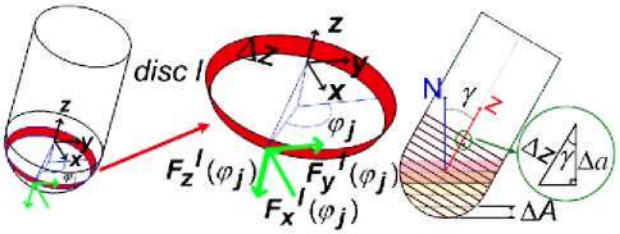

Fig. 6. Dynamic forces on the disc element l.

the tool is given in Fig. 5 for the data point 2. The full curves represent simulation results whereas curves with markers are experimental measurements. It is seen that the model predictions are in good agreement with the measurements. Distribution of the prediction error for all tests is demonstrated in Fig. 5.

3. Stability model

In the stability model, the variations of engagement and cutting conditions are taken into account by dividing the tool into disc elements with thickness of Δz (Fig. 6). The dynamic cutting forces in x, y and z directions for reference immersion angle φ on a disc element l is calculated as follows:

$$[F_x^l(\varphi) F_y^l(\varphi) F_z^l(\varphi)]^T = \Delta a \boldsymbol{B}^l(\varphi)\boldsymbol{d} \tag{1}$$

where Δa is the height of the disc elements in surface normal direction, $\boldsymbol{B}^l(\varphi)$ is the lth disc's directional coefficient matrix [8] at the reference immersion angle φ. $\boldsymbol{d}$ is the dynamic displacement vector which can be expressed as the difference between the displacements at current time and one tooth period before (Fig. 7):

$$\boldsymbol{d} = [x(t) - x(t-\tau) \quad y(t) - y(t-\tau) \quad z(t) - z(t-\tau)]^T \tag{2}$$

where τ is the tooth period. As the reference immersion angle is dependent on time, $\boldsymbol{B}^l(\varphi)$ is a time dependent periodic directional coefficient matrix. It can be represented by Fourier series expansion as follows [8]:

$$\boldsymbol{B}^l(\varphi) = \sum_{r=-\infty}^{r=\infty} \boldsymbol{B}_r^l e^{ir\varphi}, \boldsymbol{B}_r^l = \frac{1}{\varphi_p}\int_0^{\varphi_p} \boldsymbol{B}^l(\varphi) e^{-ir\varphi} d\varphi \tag{3}$$

Depending on the Fourier series expansion of the directional coefficients, there are two different stability formulation methods [8]. In the single-frequency solution, only the average of the directional coefficient matrix is used whereas in multi-frequency solution directional coefficient matrix is represented by more than one term.

3.1. Single-frequency solution

In single-frequency solution, the dynamic displacement vector is assumed to be composed of only chatter frequency ω_c. Then, it can be defined in terms of the transfer function of the structure and cutting forces [11]:

$$\boldsymbol{d} = (1 - e^{-i\omega_c\tau})\boldsymbol{G}(i\omega_c)[F_x(t) \quad F_y(t) \quad F_z(t)]^T \tag{4}$$

where $F_x(t)$, $F_y(t)$, $F_z(t)$ are total dynamic cutting forces and $\boldsymbol{G}$ is the transfer function in TCS. If Eq. (1) is written for m disc elements and summed where Eq. (4) is substituted for the dynamic displacement vector, the following eigenvalue problem is obtained:

$$[\boldsymbol{F}]e^{i\omega_c t} = \Delta a(1 - e^{-i\omega_c\tau})\left(\sum_{l=1}^{m}\boldsymbol{B}_0^l\right)\boldsymbol{G}(i\omega_c)[\boldsymbol{F}]e^{i\omega_c t} \tag{5}$$

Since the number of disc elements to be included in the analysis is not known, stability diagrams are obtained using an iterative procedure [12].

In 3-axis flat end milling, it was shown that the single-frequency solution gives good results except low radial immersion with respect to the tool diameter. However, for low radial immersion, stability diagrams were shown to be affected by multi-frequency effects [14].

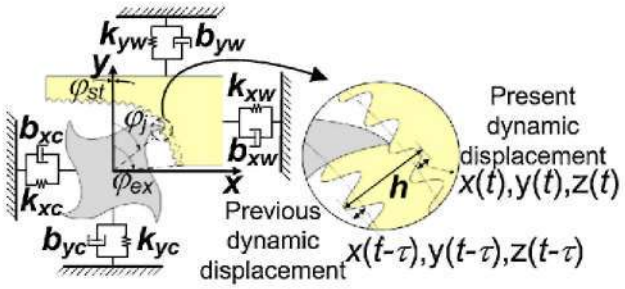

Fig. 7. The dynamic chip thickness.

3.2. Multi-frequency solution

In multi-frequency solution, higher order terms are included in the representation of directional coefficients. Multiple frequencies are addition and subtraction of the chatter frequency and harmonics of the tooth passing frequency. In this case, the dynamic displacement vector in TCS can be written in terms of the transfer function $\boldsymbol{G}$ and total dynamic cutting forces [15]:

$$\boldsymbol{d} = (1 - e^{-i\omega_c \tau}) \sum_{k=-\infty}^{k=\infty} \boldsymbol{G}(i\omega_c + ik\omega_t)\boldsymbol{F}_k e^{i(i\omega_c + k\omega_t)t} \tag{6}$$

As performed in the single-frequency solution, Eq. (1) is summed side by side for all disc elements and Eq. (6) is substituted for the dynamic displacement vector. The resulting eigenvalue problem depends on both chatter and tooth passing frequencies unlike the single-frequency solution. The numerical multi-frequency solution to obtain stability diagrams is presented in [12].

5-axis milling is used especially in finishing operations where radial depth, i.e. step over, is low. Hence, one would expect to see significant multi-frequency effects on the stability diagrams based on the observations from flat-end milling [14]. However, due to the effect of lead and tilt angles and ball-end mill geometry, these affects are suppressed in 5-axis milling. This is due to the fact that the ratio of time spent in cutting to non-cutting in 5-axis milling is higher with respect to flat-end milling. This is demonstrated in [12] by comparing the directional coefficients for flat-end milling and for ball-end milling.

3.3. Effect of machine tool kinematics configuration

The feed direction may have effect on the chatter stability if the transfer functions in two orthogonal directions are not equal. For machine tool configurations, where the rotary motions are on the tool side, lead and tilt angles do not affect the feed direction. However, if the rotary axes are on the table side, the feed vector with respect to an inertial reference frame (i.e. MCS) may become dependent on lead and tilt angles (Fig. 8a). For these cases, the measured transfer functions must be oriented considering the feed direction. The orientation of a measured transfer function $\boldsymbol{H}(i\omega_c)$ is performed using $\boldsymbol{T}_G$ matrix which depends on the lead and tilt angles, and orientation of FCN with respect to MCS [12]:

$$\boldsymbol{G} = \boldsymbol{T}_G^T \boldsymbol{H} \boldsymbol{T}_G \tag{7}$$

3.4. Stability model results

The results of the stability model are presented for a case where the workpiece material AISI 1050 steel is slotted using a 20 mm diameter ball-end mill. The modal data measured at the tool tip is given in Table 1. Firstly, the effects of lead and tilt angles on the absolute stability limit using the single-frequency method are demonstrated in Fig. 8b. For 3 lead and tilt angle combinations experimentally determined absolute stability limits are also shown. For the lead and tilt combination of (15°, −15°), the stability diagrams using single-frequency and multi-frequency methods were generated. It was observed that the measured chatter frequencies were lower than the predicted ones. This can be due to the fact that the most flexible mode presented in Table 1 is the spindle mode which was measured in idle condition, but the modal frequencies of the spindle may shift during cutting. Based on this observation, the measured frequencies under static conditions were modified in the simulations in order to match the measured chatter frequencies with the predicted ones. The simulation results using unmodified modal data with single-frequency method (hk0), modified modal data with single-frequency method (hk0_mod) and with multi-frequency method with one harmonics (hk1_mod) are presented in Fig. 9. It is seen that the simulated stability diagrams agree better with the experimental results after modified modal data is used. Furthermore, it was observed that using higher harmonics did not change the simulated stability diagrams. For the modified modal data, a time-domain model [12] was run at several spindle speeds and corresponding stability limits are presented in Fig. 9. The power spectrum of the simulated displacements is used to judge the stability of the system. There is some discrepancy between frequency-domain and time-domain results which can be attributed to the discretization procedure employed. At a stable point (A) and at an unstable point (B), power spectrums of cutting tool displacements predicted by the time-domain model are presented in Fig. 9 to be representative.

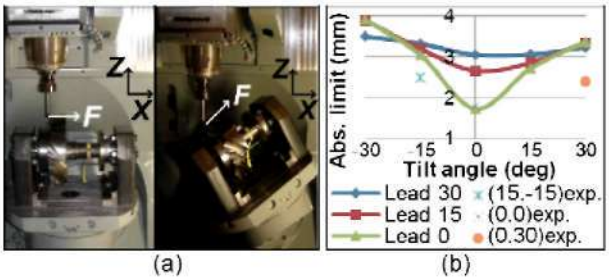

Fig. 8. Effect of lead, tilt angles on feed direction and stability.

Table 1
Modal data for the example case.

Direction	f_n (Hz)	ζ (%)	k (N/mm)
X	747.3	3.89	26,300
Y	766	3.98	36,000

4. Process simulation

For simulations, cutting geometry and conditions must be known whereas they, in general, vary continuously in 5-axis milling cycles. A practical method has been developed [13], and it is briefly described here, for identification of these parameters to simulate a full cycle.

4.1. Identification of cutting conditions

In this approach, tool orientation and position are directly obtained from the cutter location (CL) file whereas geometrical parameters, i.e. cutting depth, step over, lead and tilt angles are

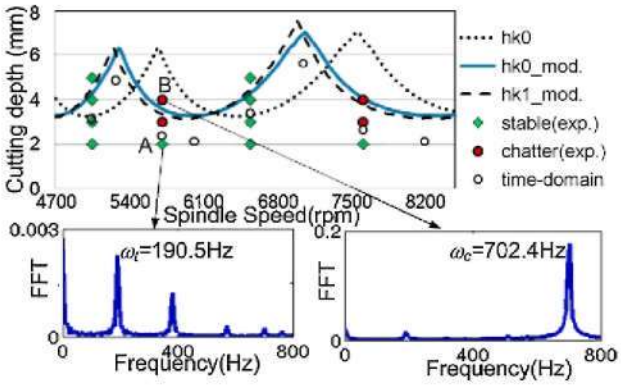

Fig. 9. Stability diagram for (15°, −15°) combination.

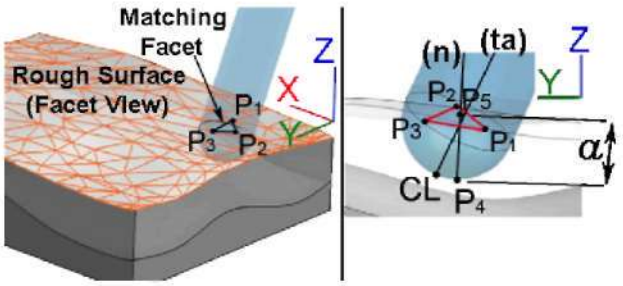

Fig. 10. Extraction of cutting depth.

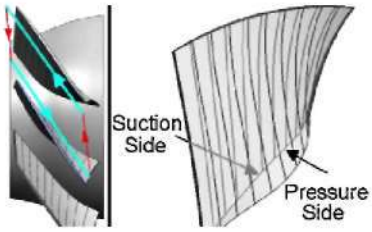

Fig. 11. Tool path pattern and workpiece geometry.

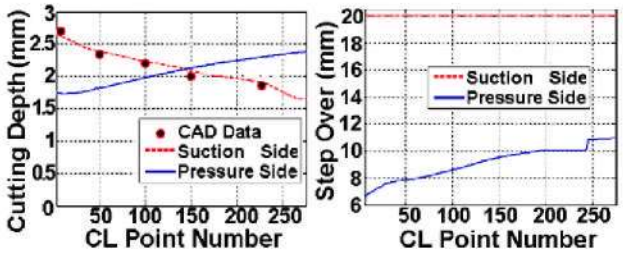

Fig. 12. Calculated cutting depth and step over.

calculated analytically [13]. Finally, the process model is used for simulations at certain CL points along the tool path. The cutting depths at each tool location in a cutting pass are determined from the relevant points on the successive tool paths as shown in Fig. 10. A *reference CL file* is generated to obtain the finished surface information, by applying 0° lead and tilt angles on the tool path. The design surface information is used in calculation of lead and tilt angles in semi-finish and finish passes, as well. In order to apply the proposed approach [13] to non-prismatic geometries (Fig. 10b), the rough workpiece information is obtained in STL format from the CAD software.

In Fig. 10, points P_1, P_2 and P_3 represent the corresponding facet of the rough surface at the given CL point. Cutting depth, a, is the distance between the points P_4 and P_5. Point P_5 is the intersection of the stock surface and the line passing through P_4 and coincident with stock surface normal (n). By analytically calculating the geometrical parameters from the CL file the process model can be used in simulation of a 5-axis cycle.

4.2. Machining of a compressor disk

A compressor blade milling process shown in Fig. 11 is analyzed using the developed method [13]. The process parameters are identified from CL files and used in force simulations, and feed scheduling. The workpiece material is Ti6Al4V. In roughing and semi-finishing cycles 20 and 16 mm diameter ball-end mills are used with feed rates of 0.16 and 0.12 mm/tooth, respectively. The lead and tilt angles are 10° and −10°. The variation of the cutting depth and the step over for the roughing pass along each side of a blade are given in Fig. 12. The analytical calculations are verified by the data from the CAD software at 5 points.

For the semi-finishing pass, F_{xy}^{max}, is simulated for every 5 CL points where there are nearly 200 points per cutting step. Calculation of the geometrical parameters for the complete blade takes 140 s whereas the force simulations for one cutting step along the blade takes 160 s on a 2.2 GHz Dual Core PC. In addition,

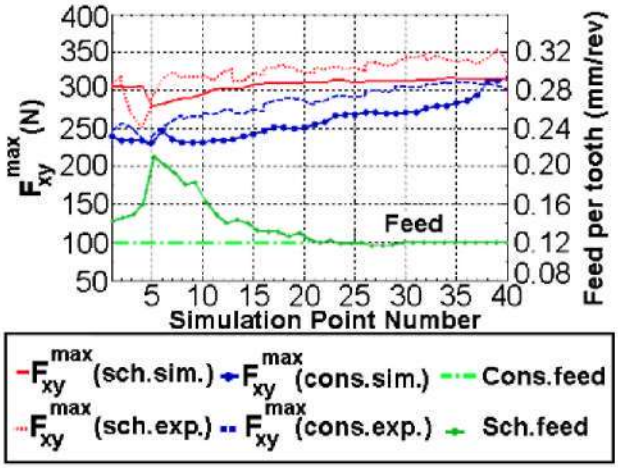

Fig. 13. Variations of F_{xy}^{max} and scheduled feed rate.

the feed is adjusted to keep F_{xy}^{max} almost constant where the step over is 2 mm. The simulated (sim.) and measured (exp.) F_{xy}^{max} for both scheduled (sch.) and constant (cons.) feed cases are shown in Fig. 13. Approximately 25% of time saving is achieved by applying feed scheduling.

5. Conclusion

The productivity and quality in 5-axis milling operations can be improved by using process models. In this paper, cutting force and chatter stability models developed for 5-axis milling are briefly introduced, and their use in selection of process parameters is demonstrated through examples. It is shown that the CL files can be used to extract parameters required for simulation of a 5-axis cycle. Using this approach, the milling forces in a cycle can be simulated, and the feed rate can be scheduled to shorten the cycle time which is demonstrated on a blade-machining example. The methods presented here can easily be integrated with CAD/CAM software for simulation of 5-axis milling operations.

References

[1] Altintas Y, Engin S (2001) Generalized Modeling of Mechanics and Dynamics of Milling Cutters. *Annals of the CIRP* 50(1):25–30.

[2] Larue A, Altintas Y (2005) Simulation of Flank Milling Processes. *International Journal of Machine Tools and Manufacture* 45:549–559.

[3] http://www.spatial.com/components/acis.

[4] Kim GM, Kim BH, Chu CN (2003) Estimation of Cutter Deflection and Form Error in Ball-end Milling Processes. *International Journal of Machine Tools and Manufacture* 43:917–924.

[5] Ozturk E, Budak E (2007) Modeling of 5-axis Milling Processes. *Machining Science and Technology* 11(3):287–311.

[6] Tlusty J, Polacek M (1963) The Stability of Machine Tools against Self-excited Vibrations in Machining. *ASME International Research in Production Engineering* 465–474.

[7] Minis I, Yanushevsky T, Tembo R, Hocken R (1990) Analysis of Linear and Nonlinear Chatter in Milling. *Annals of the CIRP* 39:459–462.

[8] Altintas Y, Budak E (1995) Analytical Prediction of Stability Lobes in Milling. *Annals of the CIRP* 44(1):357–362.

[9] Smith S, Tlusty J (1993) Efficient Simulation Programs for Chatter in Milling. *Annals of the CIRP* 42(1):463–466.

[10] Altintas Y, Shamoto E, Lee P, Budak E (1999) Analytical Prediction of Stability Lobes in Ball-end Milling. *Transactions of the ASME Journal of Manufacturing Science and Engineering* 121(4):586–592.

[11] Ozturk E, Ozlu E, Budak E (2007) Modeling Dynamics and Stability of 5-axis Milling Processes. *Proceedings of 10th CIRP Workshop on Modeling of Machining Operations*, Calabria, Italy, 469–476.

[12] Ozturk E, Budak E (2008) Chatter Stability of 5-axis Milling Using Multi-frequency Solution. *Proceedings of 3rd CIRP International Conference High Performance Cutting, vol. 1*, Dublin, Ireland, 429–444.

[13] Tunc LT, Budak E (2008) Extraction of Milling Conditions from CAM Data for Process Simulation. *International Journal of Advanced Machining Technology* . 10.1007/s00170-008-1735-7.

[14] Davies MA, Pratt JR, Dutterer BS, Burns TJ (2000) The Stability of Low Radial Immersion Milling. *Annals of the CIRP* 49(1):37–40.

[15] Budak E, Altintas Y (1998) Analytical Prediction of Chatter Stability in Milling. Part I. General Formulation; Part II. Application of the General Formulation to Common Milling Systems. *Transactions of the ASME* 120:22–36.